

## LABORATORY MEASUREMENTS OF THE ELECTRICAL PROPERTIES OF WATER ICE-SILICATE MIXTURES AND IMPLICATIONS FOR DIELECTRIC SPECTROSCOPY AND RADAR ON MARS.

D. E. Stillman and R. E. Grimm, Department of Space Studies, Southwest Research Institute, 1050 Walnut Street, Suite 300, Boulder, CO 80302, dstillman@boulder.swri.edu, grimm@boulder.swri.edu.

**Introduction:** Low frequency (1 mHz – 1 MHz) laboratory measurements of pure ice, doped ice, and regolith-ice mixtures were conducted at martian temperatures to constrain the electrical properties of water ice. These findings can then be used to optimize future electromagnetic (EM) geophysical instrument designs to search for subsurface ice on Mars. Dielectric spectroscopy (1 mHz – 10 kHz) from the martian surface can uniquely and noninvasively identify the distribution, concentration, temperature, unfrozen content, and the amount of Cl<sup>-</sup> impurities of water ice to a depth of centimeters to tens of meters. MARSIS and SHARAD are penetrating kms into the martian polar caps and imaging internal layer [1,2]. The lab measurements combined with the radar data can be used to constrain the impurity content of the ice caps as the depth of penetration is related to the electrical properties of the ice. The lab measurements can also be used to calculate the resultant reflectivity of two layers of ice with slightly different impurity content.

**Dielectric Relaxation of Ice:** Dielectric constant is a material property that describes how much more energy is stored through charge separation than in a vacuum. Charge separation is proportional to the amount of charge and the distance that the charge is moved from an equilibrium position by the application of an external electrical field. Charges of opposite signs move in opposite directions in response to an external field so that the resultant internal field between the charges opposes the external field. The charges move until the internal field cancels the external field or when the charges encounter a boundary that they cannot cross. When the external field is removed, the energy stored in this internal field decays as the charges revert back to their original positions.

Frequency dependence of dielectric constant occurs because charge separation does not happen instantaneously. Charges separate with finite velocities, thus if the external field is reversing polarity too quickly the charges cannot move fast enough to keep up. The frequency at which the charges fully separate and are in constant motion is called the relaxation frequency. At frequencies below the relaxation frequency the dielectric constant plateaus at the low frequency limit. At high frequencies above the relaxation frequency the dielectric constant plateaus at the high frequency limit.

Ice possesses a strong orientation dielectric relaxation that is caused by the migration of ionic and Bjerrum defects through the ice lattice (Fig. 1) [3]. As these defects migrate from molecule to molecule they cause the permanent electric dipole of the molecules to become rotated in such a way that the net change in polarization (internal electric field) in the ice opposes the external electric field (Fig. 1b, 1c) [3].

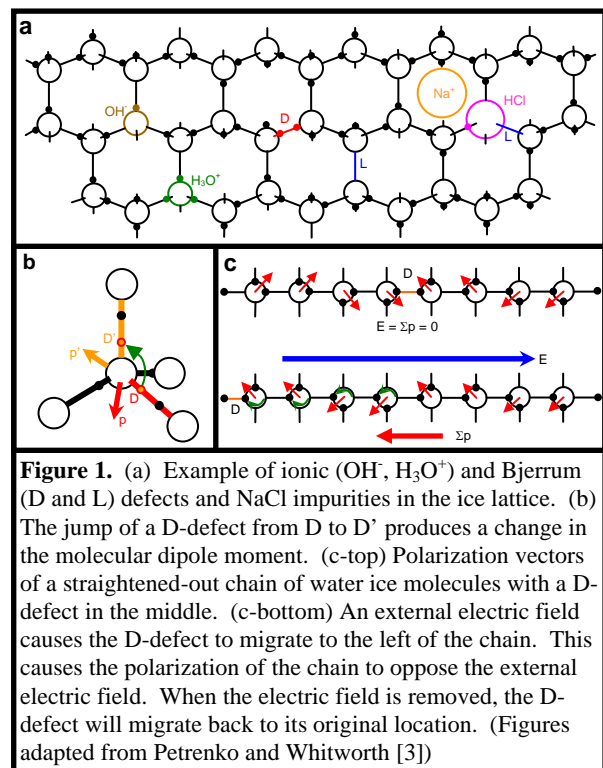


**Figure 1.** (a) Example of ionic (OH<sup>-</sup>, H<sub>3</sub>O<sup>+</sup>) and Bjerrum (D and L) defects and NaCl impurities in the ice lattice. (b) The jump of a D-defect from D to D' produces a change in the molecular dipole moment. (c-top) Polarization vectors of a straightened-out chain of water ice molecules with a D-defect in the middle. (c-bottom) An external electric field causes the D-defect to migrate to the left of the chain. This causes the polarization of the chain to oppose the external electric field. When the electric field is removed, the D-defect will migrate back to its original location. (Figures adapted from Petrenko and Whitworth [3])

The ionic and Bjerrum defects are able to migrate faster at warmer temperatures because they possess more thermal energy (Fig. 2). Cl<sup>-</sup> impurities allow these defects to migrate faster, thus also increasing the relaxation frequency. This temperature dependence of the relaxation frequency follows an Arrhenius relationship [4]

$$\tau = \tau_{\infty} e^{E/kT}$$

where:  $f_r = 1/2\pi\tau$  = relaxation frequency  
 $\tau$  = angular period of the relaxation frequency

$\tau_\infty$  = angular period of relaxation frequency at infinite temperature  
 E = activation energy  
 k = Boltzmann constant  
 T = temperature.

Decreasing temperature increases the low frequency limit of the dielectric constant by reducing the thermal energy of the defects and allowing them to stay better aligned with the electric field. Cl<sup>-</sup> impurities create more Bjerrum defects, thus increasing the low frequency limit of dielectric constant [3]. The high frequency limit of dielectric constant is not measurably dependent on temperature or impurity content and is near 3.2.

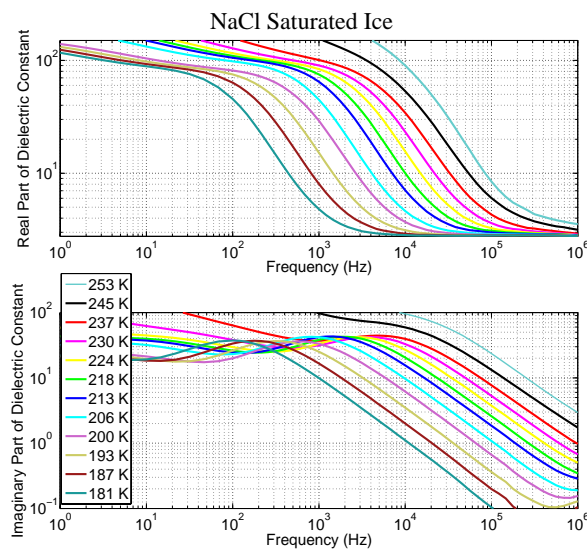


**Figure 2.** Temperature and frequency dependence of NaCl saturated ice. Low frequency limit of the real part of the dielectric constant is never attained due to the finite, static conductivity of the ice.

**Conductivity of Ice:** Static or d.c. electrical conductivity is a material property that describes the energy lost due to the migration of unbound charges. The difference between conductivity and dielectric constant is that once the external electric field is removed the charges do not return to their previous location. Static conductivity is equivalent to the reciprocal of static resistivity.

The static conductivity of ice is extremely sensitive to impurities. There is no evidence that the conductivity of an impurity free ice has ever been measured [3]. Even with a very small amount of impurities, ice still has a greater conductivity than dry rock or regolith. The static conductivity occurs as ions from impurities migrate at grain boundaries. Close to the melting point, liquid water may still persist due to capillary

forces [5]. The ability of ions to move in these unfrozen water films will determine their ability to influence radar sounding [6], geochemistry [7], and microbial habitats [8,9].

**Laboratory Apparatus:** The dielectric relaxation of pure and doped ice has been measured previously; however much uncertainty remains as many of the measurements disagree [10,11,12,13]. Little research has been conducted on the effects of ice in soil [14,15]. To reduce this uncertainty, temperature and frequency dependent electrical property measurements of pure ice, doped ice, and regolith-ice mixtures have been measured over a temperature range from 180 – 273 K and frequency range from 1 mHz – 1 MHz. Electrical property measurements are made using a 1260 Solartron Impedance Analyzer connected to a 1296 Solartron Dielectric Interface. The sample is placed in a parallel plate capacitor consisting of three electrodes (anode, cathode, and ground). When current is injected, the sample and its holder act as a resistor (proportional to the static conductivity) and lossy capacitor (proportional to the dielectric constant) in parallel. The Solartron measures complex impedance versus frequency; this is converted into electrical properties by using the geometry of the three-electrode sample holder. Electrical properties can be expressed as complex dielectric constant, complex conductivity, or complex resistivity.

**Laboratory Procedure:** The regolith is dried at 383 K overnight for low surface area regolith and at 383 K several days for high surface area regolith before saturating the regolith with water. The sample is added to the sample holder and is quickly lowered below freezing. Humidity is maintained in the test chamber to minimize evaporation of water from the sample. Below freezing, the temperature of the sample is slowly lowered (0.1 K/min) to the desired temperature to minimize any cracking. Once at the desired temperature ( $\pm 0.5$  K), multiple measurements are made to monitor any change in the sample over time. Typically the sample's electrical properties change over the course of many hours because ice is always trying to minimize its grain boundary energy which causes the ice crystals to grow during this time.

**Laboratory Results:** The results of our dielectric measurements of pure ice closely match those of Johari and Jones [13] (Fig. 3). They also confirm that ice doped with Cl<sup>-</sup> possesses a much higher relaxation frequency, and that once Cl<sup>-</sup> saturates the ice lattice at  $\approx 10^{-5}$  M the Cl<sup>-</sup> no longer affects the dielectric properties of the sample. The JSC Mars-1 ice mixture shows an increase in the relaxation frequency which is most

likely caused by a small amount ( $<10^{-6}$  M) of  $\text{Cl}^-$  impurities that were dissolved off the JSC Mars-1 grains. The glass beads ice mixture shows a stronger increase in the relaxation frequency which is most likely caused by a  $\gg 10^{-5}$  M concentration of  $\text{Cl}^-$  impurities that were dissolved off the glass beads grains. Therefore these measurements showed that our regolith-ice mixtures did not change the relaxation frequency of the ice. This contradicts the findings of Alvarez [14,15].

Temperature Dependence of Relaxation Frequency

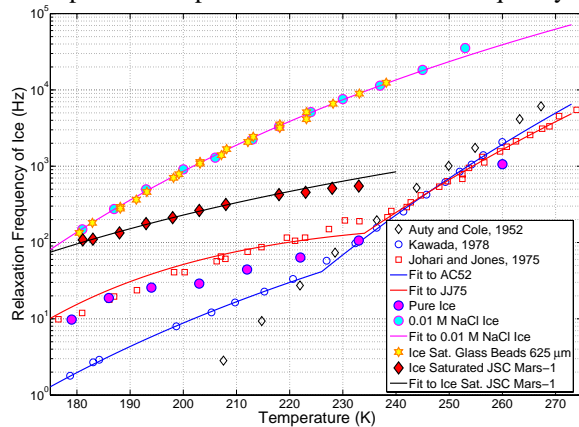


**Figure 3.** Previous measurements (open symbols) and our measurements (closed symbols) of the temperature dependence of the relaxation frequency.

Static conductivity measurements of regolith-ice mixtures show that the conductivity is controlled by the impurity content of the ice (Fig. 4). The only exception to this is the large jump in conductivity in the glass beads sample near 255 K. This was repeatable and is believed to be caused by a freezing depression of water due to high  $\text{Cl}^-$  concentration. No electrical effects of unfrozen films of water were observed below  $-5^\circ\text{C}$ . However, NMR data demonstrate that unfrozen water persists in these samples to at least  $-40^\circ\text{C}$  [16].

Temperature Dependence of Static Conductivity

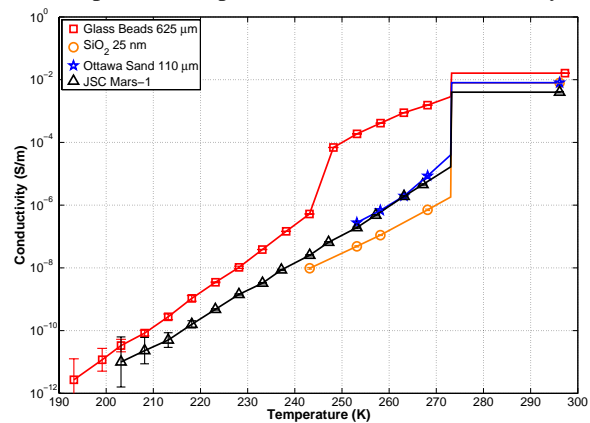


**Figure 4.** Static conductivity of ice-silicate mixtures. All samples show similar frequency dependence (activation energy), suggesting conductivity is dominated by impurities along ice grain boundaries without regard to silicate abundance or composition.

**Applications for Dielectric Spectroscopy:** Narrowband measurement of the resistive-capacitive properties of the earth (known as induced polarization or IP in geophysics) has been used for nearly a century to explore for minerals and groundwater and to characterize subsurface geology. Broadband systems are now seeing wide application, including environmental studies [e.g., 17]. The Huygens, the Rosetta lander, and Phoenix spacecraft all include electrical-properties sensors and Hamelin [18] discussed making measurements similar to this on Mars.

Dielectric spectroscopy injects a sinusoidal current into two current electrodes while measuring the resultant potential difference between two potential electrodes. Depth of investigation scales with electrode separation: electrodes mounted on lander footpads or rover wheels would sense to depths of a few tens of centimeters, whereas a ballistically deployed electrode string could probe ten meters or more into the subsurface (Fig. 5). A string of electrodes has the additional advantage of being able to form a true cross-section due to the numerous current-potential geometries. The characterization of the full bandwidth of possible water ice responses and soundings to depths of meters or more requires high-impedance ( $\sim 10$  T $\Omega$ ), low-capacitance ( $\sim 1$  pF) coupling, mitigation of coherent noise such as leakage and eddy currents using buffering shielding, guarding of electrodes, and larger electrode arrays. Our present efforts are aimed toward a design of transmitter and receiver requiring a few kilograms and a few watts, plus sensors.

Unlike neutron spectroscopy, this method is not limited to the top tens of centimeters and it will not be susceptible to dry hydrated minerals. A forward calcu-

lation using present estimates of the intrinsic properties of ice and its moderation due to regolith mixing (Fig. 6) illustrates that an ice-detection limit of ~1% or better is possible.

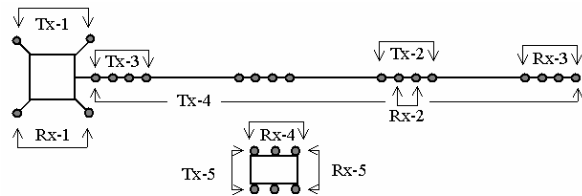


**Figure 5.** Alternative schematic layouts for IP electrodes. Tx = transmitter, Rx = receiver. (1) Electrodes on static lander footpads. (2) Closely spaced electrodes on ballistically deployed string for shallow subsurface investigation. (3) Widely spaced electrodes for deeper investigation. (4) Large transmitter dipole on lander and short dipole on rover (wheel base) for deep investigation. (5) Rover-only short dipoles for mobile, shallow investigation.

#### Applications for Ground Penetrating Radar:

The orbital ground penetrating radars of MARSIS (1.3-5.5 MHz) and SHARAD (15-25 MHz) have imaged the base and many internal reflectors of the martian polar caps. The low attenuation rate (1 – 4 dB/km [2]) of these caps is controlled by the electrical properties of the ice. These are a function of the impurity content, temperature, and dust content. This makes solving for just the impurity content non-unique, however as more is learned about the martian polar caps better estimates could be made.

The internal reflections could be caused by differing concentrations of impurities that would change the conductivity and complex dielectric constant of the ice. Our measurements could be extrapolated to at least 25 MHz because real part of dielectric constant is usually frequency independent at this frequency range because of its cold temperature. The measurements could then be used to construct to reflectivity strength of layers of differing impurities similar to Nunes and Phillips method with dust concentration [19]. Understanding the concentration of impurities is important because it influences the grain size and rheology of ice, which are important factors in determining flow in the caps.

**Acknowledgements:** This work was supported by NASA Exobiology Research award no. NNG05GN16G and NASA Mars Fundamental Research award no. NNG05GL88G. The authors thank Steve Dec for NMR results and Mark Bullock, Amy Barr, and Joe MacGregor for useful discussions.

**References:** [1] Picardi, G. et al., (2005), *Science*, 310, 1925-1928. [2] Plaut, J.J. et al., (2007), *Science*, 316, 92-95. [3] Petrenko V.F. and Whitworth R.W. (1999) *Physics of Ice*, 373 pp. [4] Kauzmann, W. (1942) *Rev. Mod. Phys.*, 14, 12-44. [5] Davis, N. (2001) *Permafrost*, Univ. Alaska. [6] Grimm, R.E. (2002) *JGR*, 107, 10.1029/2001JE001504. [7] Landis G.A. (2004) LPSC XXV, #2188. [8] Jakosky, B.M. et al. (2003) *Astrobiology*, 3, 343. [9] Jepsen, S.M. et al. (2007) *Astrobiology*, in press. [10] Auty, R.P. and Cole R.J. (1952) *J. Chem. Phys.*, 20, 1309. [11] Johari, G.P. and Jones J. (1975) *J. Chem. Phys.*, 62, 4213. [12] Kawada, S. (1978) *J. Phys. Soc. Jpn.*, 44, 1881-1886. [13] Johari G.P. and Whalley E. (1981) *J. Chem. Phys.*, 75, 1333-1340. [14] Alvarez R. (1973) *Earth & Planet. Sci. Lett.*, 20, 409-414. [15] Alvarez R. (1973) *Science*, 179, 1122-1123. [16] Grimm, R.E. et al. (2006) LPSC XXXVIII, #2249. [17] Grimm, R.E. (2005) *J. Environ. Eng. Geophys.*, 10, 351-364. [18] Hamelin, M. et al. (2003) *JGR*, 108, 10.1029/2002JE001893. [19] Nunes, D.C. and Phillips, R.J., (2006), *JGR*, 111, E06S21 [20] Telford W.M. et al. (1990) *Applied Geophysics*, 770 pp. [21] Carrier, W.D. (1991) in *Lunar Sourcebook* (eds. Heiken et al.), 475-594.

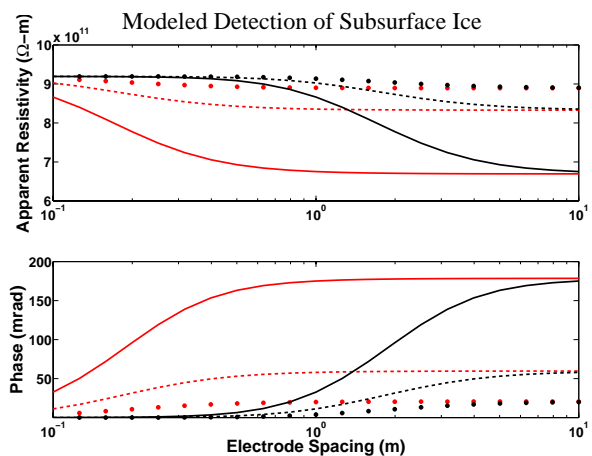


**Figure 6.** Forward models for the geoelectrical signature of ice from surface electrode arrays. Model invokes a two-layered structure [20], uses the complex refractive index model (CRIM) to calculate electrical properties of mixtures of soil and the target substance, and assumes that multiple electrodes are distributed along a linear antenna such that four-electrode combinations can be used at a variety of spatial scales. Ice depths of 0.1 m (red) and 1 m (black) and ice fractions 10% (solid), 3% (dash), and 1% (dot) indicate that ice can be resolved at percent abundance or better (relaxation time constant of ice after Kawada [12]; dry regolith resistivity 10<sup>12</sup> Ω-m after Carrier et al. [21]; test frequency 10 Hz).